Cancer Therapy: Preclinical

Clinical Cancer Research

The Investigational Aurora Kinase A Inhibitor MLN8237 Induces Defects in Cell Viability and Cell-Cycle Progression in Malignant Bladder Cancer Cells *In Vitro* and *In Vivo*

Ning Zhou[1], Kamini Singh[2], Maria C. Mir[1], Yvonne Parker[5], Daniel Lindner[5], Robert Dreicer[5], Jeffrey A. Ecsedy[6], Zhongfa Zhang[7], Bin T. Teh[8], Alexandru Almasan[2], and Donna E. Hansel[1,3,4,5]

Abstract

Purpose: Despite more than 70,000 new cases of bladder cancer in the United States annually, patients with advanced disease have a poor prognosis due to limited treatment modalities. We evaluated Aurora kinase A, identified as an upregulated candidate molecule in bladder cancer, as a potential therapeutic target.

Experimental Design: Gene expression in human bladder cancer samples was evaluated using RNA microarray and quantitative reverse transcriptase PCR. Effects of the Aurora kinase A inhibitor MLN8237 (Millennium) on cell dynamics in malignant T24 and UM-UC-3 and papilloma-derived RT4 bladder cells were evaluated *in vitro* and *in vivo* in a mouse xenograft model.

Results: A set of 13 genes involved in the mitotic spindle checkpoint, including Aurora kinases A and B, were upregulated in human urothelial carcinoma compared with normal urothelium. The Aurora kinase A inhibitor MLN8237 induced cell-cycle arrest, aneuploidy, mitotic spindle failure, and apoptosis in the human bladder cancer cell lines T24 and UM-UC-3. MLN8237 also arrested tumor growth when administered orally over 4 weeks in a mouse bladder cancer xenograft model. Finally, *in vitro* sequential administration of MLN8237 with either paclitaxel or gemcitabine resulted in synergistic cytotoxic effects in T24 cells.

Conclusions: Mitotic spindle checkpoint dysfunction is a common characteristic of human urothelial carcinoma and can be exploited with pharmacologic Aurora A inhibition. Given our demonstration of the ability of the Aurora A inhibitor MLN8237 to inhibit growth of bladder cancer *in vitro* and *in vivo*, we conclude that Aurora kinase inhibitors warrant further therapeutic investigation in bladder cancer. *Clin Cancer Res; 19(7); 1717–28. ©2013 AACR.*

Introduction

The Aurora kinases comprise a family of serine/threonine kinases that play an essential role in cell-cycle progression, most notably during the G_2 and M phases. Three human homologs, Aurora kinases A, B, and C, have been characterized and maintain discrete functions within the cell cycle. Aurora A participates in centrosome assembly/maturation and proper function of the mitotic spindle apparatus, and thus is critical for the maintenance of genomic integrity (1–3). Aurora B localizes to the mitotic kinetochore and the mid-body of cytokinesis and facilitates function of the mitotic spindle checkpoint complex, histone-H3 phosphorylation, and cytokinesis (4). Aurora C expression is localized to the testes and is purported to overlap somewhat with Aurora B function in facilitating spermatogenesis although its exact functions remain unclear (5, 6).

While the involvement of Aurora C in cancer development remains uncertain, Aurora A and B have been frequently implicated in human carcinogenesis. Both overexpression and gene amplification of Aurora A have been characterized in human tumors and have been shown to correlate with tumor proliferation rates and prognostic markers (7–13). Indeed, forced overexpression of Aurora A can induce malignant transformation through dysregulation of mitotic processes, including the mitotic spindle checkpoint and promotion of chromosomal instability (14–16). Overexpression of Aurora B is also an established characteristic of certain human cancers, and exogenous

Authors' Affiliations: [1]Pathology and Laboratory Medicine Institute; [2]Lerner Research Institute; [3]Glickman Urological and Kidney Institute; [4]Genomic Medicine Institute; [5]Department of Solid Tumor Oncology, Cleveland Clinic, Cleveland, Ohio; [6]Millennium Pharmaceuticals, Cambridge, Massachusetts; [7]Van Andel Research Institute, Grand Rapids, Michigan; and [8]NCCS-VARI Translational Research Laboratory, National Cancer Center, Singapore, Singapore

Note: Supplementary data for this article are available at Clinical Cancer Research Online (http://clincancerres.aacrjournals.org/).

Corresponding Author: Donna E. Hansel, Pathology and Laboratory Medicine Institute, Cleveland Clinic, Desk L25, Cleveland, OH 44195. Phone: 216-444-5893; Fax: 216-445-3707; E-mail: hanseld@ccf.org

doi: 10.1158/1078-0432.CCR-12-2383

Translational Relevance

Despite poor outcomes for patients receiving chemotherapy, bladder cancer remains a relatively understudied disease with little advancement in nonsurgical treatment modalities in the last few decades. We sought to identify pathways in human bladder cancer that could be exploited with targeted therapies, leading us to identify mitotic spindle checkpoint dysfunction and to evaluate the effects of the Aurora kinase A inhibitor MLN8237 in bladder cancer. While Aurora kinase overexpression has been previously described in bladder cancer, to our knowledge, this study represents the first preclinical evaluation of aurora kinase inhibitors specifically for bladder cancer. On the basis of our mechanism-based hypothesis of the efficacy of Aurora kinase inhibition in bladder cancer, as well as our validation of *in vitro* findings using a mouse xenograft study and our demonstration of schedule-dependent synergistic effects between MLN8237 and gemcitabine and paclitaxel, we feel strongly that this pathway warrants further therapeutic investigation in bladder cancer.

overexpression of Aurora B is also capable of promoting tumor cell invasiveness in animal models (17–19). In human urothelial carcinoma of the bladder, increase in copy number and expression levels of Aurora A and B have been reported to correlate with pathologic and clinical parameters, including tumor grade and prognostic significance (7–9, 20).

The critical roles of Aurora A and B in mitotic progression and their shown oncogenic potential have prompted the development of Aurora kinase inhibitors as targeted anticancer agents. Several small-molecule inhibitors of Aurora kinases have been developed and are currently undergoing preclinical and early clinical testing. In particular, MLN8237 is a novel, orally bioavailable, second-generation selective inhibitor of Aurora A. MLN8237 and its predecessor MLN8054 have exhibited efficacy against solid tumors and hematologic malignancies in preclinical models and are currently undergoing evaluation in hematologic and solid cancers (21–26).

Despite bladder cancer being the fourth most common cancer in men with more than 70,000 new cases annually in the United States, patients with advanced disease have a poor prognosis irrespective of current surgical and chemotherapeutic treatment options, with 5-year survival rates around 20% or lower for surgically incurable patients (27–30). For patients with locally advanced and/or metastatic disease, combination chemotherapy regimens are commonly used, although only a small subset of patients with advanced disease is cured and minimal progress has been made in developing new therapies (28–31). Thus, alternative and/or complimentary targeted therapy for these patients may be of value in prolonging survival. In this study, we use gene expression analysis to show that components of the mitotic spindle checkpoint, including Aurora kinases A and B, are broadly dysregulated in human bladder cancer. We hypothesize that this can be exploited therapeutically with Aurora kinase inhibition, and we test the antitumor activity of the selective Aurora A inhibitor MLN8237 *in vitro* in bladder cancer cell lines and *in vivo* in a mouse xenograft model. To our knowledge, this study is the first to evaluate Aurora kinase inhibitors specifically for bladder cancer.

Materials and Methods

Gene expression analysis

Snap-frozen human samples of normal urothelium ($N = 10$) and muscle-invasive urothelial carcinoma of the bladder ($N = 8$) were subjected to RNA microarray using the Affymetrix Hgu133plus2 gene array platform (Affymetrix) according to manufacturer's instructions. Normal urothelium was obtained from distal ureteral samples from patients with renal cell carcinoma and no history of prior urothelial neoplasia. Ten micrograms of total RNA was processed for the expression microarrays using the Affymetrix GeneChip One-Cycle Target Labeling Kit (Affymetrix) according to the manufacturer's recommended protocols. The resultant biotinylated cDNA was fragmented and then hybridized to the GeneChip human genome (54,675 probe sets in total, including more than 35,000 human genes; Affymetrix). The arrays were washed, stained, and scanned using the Affymetrix Model 450 Fluidics Station and Affymetrix Model 3000 scanner using the manufacturer's recommended protocols.

Expression values were generated by using Microarray Suite (MAS) v5.0 software (Affymetrix). The probes were redefined using updated probe set mappings (Bioc package: hs133phsentrezgcd; ref. 32). The hybridizations were normalized using the robust multichip averaging (rma) algorithm implemented in Bioconductor package affy (http://www.bioconductor.org/; ref. 33) to obtain a summary expression value for each probe set of genes (34–36). This resulted in a gene expression intensity dataset containing more than 17,000 rows (genes), each of which has 1 numeric value representing its relative expression intensity in the sample.

Gene expression levels were summarized according to the genes' physical locations using the regional expression biases package in Bioconductor (34, 35). The algorithm groups the gene expression intensities by the associated gene locations. For each region (cytoband), a general test (such as binomial or *t* test) is applied to determine if the gene expressions in the region are collectively higher or lower than the reference expressions. The test statistics are then output for each sample and for each cytogenetic region.

Two-step quantitative reverse transcriptase PCR (qRT-PCR) was also conducted on normal urothelium ($N = 3$) and invasive bladder cancer ($N = 3$) samples using the Superscript III First-Strand Synthesis System (Invitrogen) according to manufacturer's instructions and SYBR

Green qPCR MasterMix (Applied Biosystems). Twenty-five microliter reactions (1× SYBR Green Master Mix, 100 pmol/L forward primer, 100 pmol/L reverse primer, and 100 nmol/L cDNA) in duplicate were run on ThermoGrid 96-well polypropylene PCR plates (Denville Scientific) using a 7500 Real Time PCR System (Applied Biosystems). Results were analyzed using 7500 System SDS Software v1.4 (Applied Biosystems), and *t* test was used to analyze differences in expression level between normal urothelium and invasive bladder cancer. The reaction was as follows: 50°C for 2 minutes, 95°C for 10 seconds, (95°C for 15 seconds, 60°C for 1 minute) × 50 cycles. PCR primers were as follows: AURKA: f:5′-tggaatatgcaccacttgga-3′; r:5′-actgaccacccaaaatctgc-3′; AURKB: f:5′-gggagagctgaagattgctg-3′; r:5′-ggcgataggtctcgttgtgt-3′; BUB1B: f:5′-agccagaacagaggactcca-3′; r:5′-tgaagctgtattgccacgag-3′; CCNA2: f:5′-ttattgctggagctgccttt-3′; r:5′-ctctggtgggttgaggagag-3′; CDC2: f:5′-ccatggggattcagaaattg-3′; r:5′-ccatttttgccagaaattcgt-3′; DLG7: f:5′-ggaagaattcctttgcacct-3′; r:5′-ccaaaggacatggcaattta-3′; MAD2L1: f:5′-gtggtgaggtcctggaaaga-3′; r:5′-ccgactcttcccatttttca-3′; NUF2: f:5′-gaaaaacttgccacagcaca-3′; r:5′-tccctttcagcagcatcttt-3′; TPX2: f:5′-tggaaatatgccctttctcg-3′; r:5′-gcttccaagtctgtgccttc-3′; KIF11: f:5′-atgctggtgtggattgttca-3′; r:5′-tcaagttctggggtttcagg-3′; KIF4A: f:5′-gtcagaatggagcaacagca-3′; r:5′-acctggaggagggtcagttt-3′; ZWINT: f:5′-aggcaattgcagctaaggaa-3′; r:5′-actgctctgcgtttctccat-3′; GAPDH: f:5′-gtcagtggtggacctgacct-3′; r:5′-aggggtctacatggcaactg-3′.

Cell culture and drug treatments

Human urothelial carcinoma cell lines T24, UM-UC-3, and RT4 were purchased from the American Type Culture Collection and cultured at 37°C and 5% CO_2 in RPMI-1640 media (Gibco) supplemented with 10% FBS (Gibco). Drugs evaluated included the Aurora kinase A inhibitor MLN8237 (a kind gift from Millennium Pharmaceuticals), paclitaxel (Sigma), and gemcitabine (Sigma). MLN8237 and paclitaxel were diluted in dimethyl sulfoxide (DMSO; Sigma) and gemcitabine was diluted in sterile water. For *in vitro* administration of drugs, aliquots of 10 mmol/L working solutions of each drug were stored at −20°C until use. Media changes were carried out 1 day before drug addition and drugs were added directly to the culture media when cells reached 25% to 50% confluency.

Flow cytometry

For cell-cycle analysis, treated cells were trypsinized, pelleted, and fixed in a 70% ethanol/30% PBS v/v solution at 4°C. Samples were stained with 50 μg/mL propidium iodide (PI; Santa Cruz Biotechnology) in 0.05% Triton-X-100 and 1× PBS for 2 hours at room temperature before acquisition. For annexin V staining for analysis of apoptosis, cells were trypsinized, harvested, and stained with annexin V and PI using the FITC Annexin V Apoptosis Detection Kit I (BD Pharmigen) according to manufacturer's instructions. Cells were analyzed on a Becton-Dickinson FACScan flow cytometer (Becton-Dickinson) with ModFIT LT software (Verity Software House).

Western blot analysis

Antibodies used included mouse anti-Aurora A (1:1,000; Abcam), rabbit anti-histone H3 (1:500; Abcam), rabbit anti-P-Aurora A-T288 (1:500; Cell Signaling Technologies), rabbit anti-P-histone-H3 (1:500; Cell Signaling Technologies), rabbit anti-cleaved PARP (1:1,000; Cell Signaling Technologies), rabbit anti-p73 (1:500; Bethyl Laboratories), rabbit anti-p53 (1:500; Cell Signaling Technologies), rabbit anti-p21 (1:500; Abcam), and rabbit anti-β-actin (1:2,000; Thermo Sci). Western blot analyses were conducted according to standard procedures and as previously detailed (37). Blots were blocked with 1% bovine serum albumin (BSA) diluted in TBS-T for P-Aurora A-T288 and P-histone-H3 antibodies, or in 5% Carnation instant milk in TBS-T for remaining antibodies, for 1 hour at room temperature. Blots were incubated with primary antibody overnight at 4°C in blocking solution and rinsed with TBS-T, followed by incubation for 2 hours at room temperature with alkaline phosphatase–conjugated anti-rabbit immunoglobulin G (IgG; 1:10,000; Sigma) or anti-mouse IgG (1:10,000; Sigma) antibody and visualized using the Enhanced Chemiluminescence Kit (Amersham). Blots were scanned for chemifluorescence using a Molecular Dynamics Typhoon 8600 Variable Mode Imager (Amersham).

Immunocytochemical staining

Cells grown on coverslips were fixed with 100% methanol at 4°C for 15 minutes. Cells were blocked with 1% BSA (Sigma) in PBS-T (PBS-0.25% Tween) for 1 hour at room temperature. Cells were incubated with primary antibodies diluted 1:50 in 1% BSA–PBS-T overnight at 4°C, rinsed with PBS-T, and incubated with secondary antibodies diluted 1:1,000 in 1% BSA–PBS-T for 2 hours at room temperature. Antibodies used included rabbit anti-β-tubulin (Sigma), mouse anti-tubulin (Sigma), mouse anti-Aurora A (Abcam), rabbit-anti-P-Aurora A-T288 (Cell Signaling Technology), rabbit anti-CENP-A (Cell Signaling Technology), rabbit anti-Cy3 (Thermo Sci), and mouse anti-Cy5 (Thermo Sci).

Fluorescence, phase-contrast, and time-lapse microscopy

Cells grown on coverslips were stained with 4′,6-diamidino-2-phenylindole (DAPI; Sigma) at 1 μg/mL for 15 minutes at room temperature. Coverslips were mounted in 50% glycerol/PBS v/v, and imaged using a Leica DMR Upright microscope (Leica) with a Retiga EX Cooled CCD camera (Regita) and Image-Pro Plus software (Media Cybernetics). Phase-contrast microscopy was conducted using the same camera setup on cells grown on coverslips and fixed as previously described without any additional staining procedures conducted. For live cell time-lapse microscopy, cells were plated in 6-well plates, treated with MLN8237 or DMSO, imaged for 48 hours with phase-contrast images taken every 10 minutes using a Leica DMIRB Inverted microscope (Leica) with CoolSNAP HQ Cooled CCD camera (Princeton Instruments), and processed using LAS-AF (Leica) software.

Clonogenic assay

To determine clonogenic survival following treatment, cells treated for 48 hours were trypsinized, counted by hemocytometer, and replated at a concentration of 200 cells per 10-cm tissue culture plate. After 8 days to allow clones to form in T24 cells and 15 days in RT4 cells (due to inherent differences in mitotic rate), plates were fixed with 100% methanol at 4°C for 5 minutes, stained with 0.5% crystal violet for 5 minutes, and washed 3 times with 1× PBS.

In vitro assessment of drug interactions

Cells were plated into 96-well plates at 1,000 cells per well and drugs were added into culture media as previously described. To evaluate drug interactions, MLN8237 was combined with either paclitaxel or gemcitabine. Drugs were administered either simultaneously for 48 hours, or sequentially, with one drug for 48 hours, followed by 3 washes with 1× PBS and immediate addition of the second drug for 48 hours. All drugs were administered at several concentrations and all treatments were carried out in triplicate. To assess cytotoxic effects, CellTiter96 AQueous Cell Proliferation assay (Promega), a MTS-based assay, was conducted according to manufacturer's instructions. The 96-well plates were measured for absorbance using a Wallac 1420 Victor Plate Reader (Wallac). Given the linearity of this assay, samples were expressed as a ratio of their absorbance at 490 nm to the absorbance at 490 nm of an untreated control sample. Drug–drug interactions and combination indices were measured using CalcuSyn (Biosoft) and the Chou-Talalay median-effect method (38). Combination indices less than 0.5 were defined as synergistic interactions and combination indices greater than 1.5 were defined as antagonistic interactions. To assess cell viability, cells plated and treated in 96-well plates as described earlier were washed with 1× PBS, trypsinized and harvested, stained with 10% Trypan blue (Sigma), and counted with a hemacytometer.

In vivo mouse xenograft model

In vivo antitumor capacity of MLN8237 was evaluated in a mouse xenograft model of bladder cancer. For inoculation, 10^6 T24 cells in 50% Matrigel were injected into the flanks of nude mice bilaterally. Mice were divided into either the treatment group or the control group, with 8 tumors per group. MLN8237 was administered at 30 mg/kg by oral gavage 5 times weekly for 4 weeks. Mice in the control group received vehicle only. Tumors sizes were measured 3 times weekly. Tumor volumes were calculated by the following formula: $0.5 \times (\text{smaller dimension})^2 \times (\text{larger dimension})$. At the completion of treatment, mice were sacrificed and tumors flash-frozen for staining.

Staining of mouse xenograft tumors

To evaluate proliferation in mouse xenograft tumors, frozen tissue sections were thawed and fixed with 2.0% paraformaldehyde/PBS for 15 minutes at room temperature, washed 3× for 10 minutes each, permeabilized with 0.1% Triton X-100 in PBS for 5 minutes, and blocked in 10% FBS in PBS for 1 hour. Immunostaining was carried out using anti-Ki67 diluted in blocking buffer, followed by fluorescently conjugated secondary antibody. DAPI was added before penultimate washing to stain nuclei. To evaluate cell death, paraffin-embedded tissue sections were dewaxed and rehydrated according to standard serial xylene and ethanol wash protocols and permeabilized with a 0.1% Triton X-100, 0.1% sodium citrate solution for 10 minutes. Slides were then stained using the In Situ Cell Death Detection Kit Fluorescein (Roche Applied Science) according to manufacturer's instructions. For imaging, slides were mounted in Vectashield (Vector Laboratories, H-1000), and images were collected using a Leica DMR Upright microscope (Leica) with a Retiga EX Cooled CCD camera (Regita) and Image-Pro Plus software (Media Cybernetics).

Results

Mitotic spindle checkpoint genes are overexpressed in invasive urothelial carcinoma

Initial evaluation of gene expression profiles in human bladder cancer identified a general upregulation of multiple mitotic spindle genes, including Aurora kinase A. Specifically, RNA microarray using the Affymetrix Hgu133plus2 gene array platform was conducted on human specimens of high-grade urothelial carcinomas of the bladder ($N = 10$) and normal urothelium ($N = 8$). This screen identified 155 genes differentially expressed at least 5-fold in the urothelial carcinoma samples compared with normal urothelium, which notably included a subset of 13 overexpressed genes with roles within the mitotic spindle checkpoint (Fig. 1A). Among the transcripts overexpressed in urothelial carcinoma were Aurora A (5.6-fold increased expression) and Aurora B (6.2-fold); MAD2L1 (7.6-fold) and BUB1B (8.8-fold), 2 primary components of the APC/C inhibitory complex; TPX2 (9.3-fold), which interacts with Aurora A; the mitotic spindle kinesin KIF11 (7-fold); and the mitotic regulator CDC20 (11.4-fold). These data have been deposited in National Center for Biotechnology Information's (NCBI) Gene Expression Omnibus (GEO) and are accessible through GEO Series accession number GSE42089 (http://www.ncbi.nlm.nih.gov/geo/query/acc.cgi?acc=GSE42089; 39).

qRT-PCR on a separate set of human urothelial carcinomas and normal urothelium re-affirmed overall upregulation of these spindle checkpoint genes, with 10 of 13 genes showing statistically significant differential expression levels (Fig. 1B). Thus, mitotic spindle checkpoint transcripts seem to be broadly upregulated in human urothelial carcinoma of the bladder. Given the function of Aurora A in mitotic progression and its shown oncogenic potential in other cancers, we next focused on the potential of Aurora A as a therapeutic target in bladder cancer.

MLN8237 selectively inhibits Aurora A and induces cell-cycle arrest and aneuploidy in bladder cancer cell lines

We used the Aurora A–specific inhibitor MLN8237 to evaluate the effects of Aurora A inhibition on the

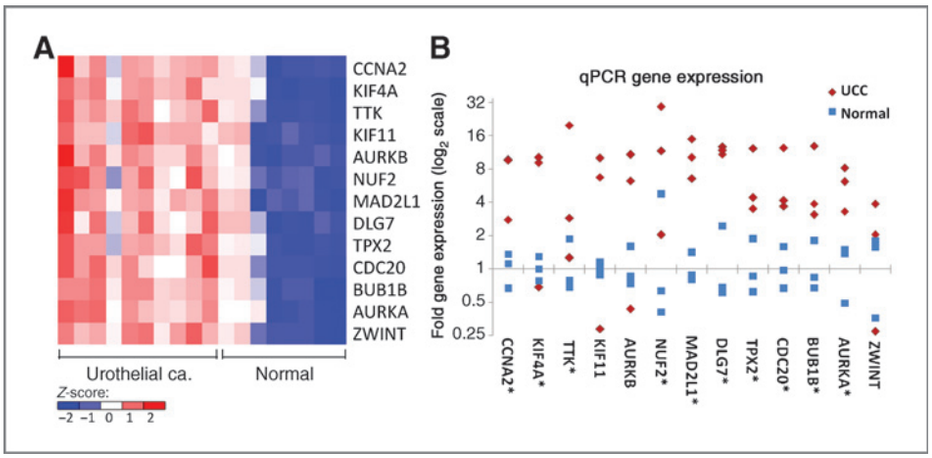

Figure 1. Mitotic spindle checkpoint genes are broadly overexpressed in human urothelial carcinoma. A, human samples of normal urothelium ($N = 10$) and urothelial carcinoma of the bladder ($N = 8$) were subjected to RNA microarray. A subset of 13 gene transcripts related to the mitotic spindle checkpoint, including Aurora A and B, were upregulated at least 5-fold in the urothelial carcinoma (UCC) compared with the normal urothelium. B, upregulation of these genes was validated by 2-step quantitative real-time PCR on a separate set of human samples of urothelial carcinoma ($N = 3$) and normal urothelium ($N = 3$). Ten of 13 genes (asterisked) showed statistical significance (*t* test; $P < 0.05$) for differential expression in urothelial carcinoma compared with normal urothelium.

human urothelial carcinoma cell lines T24 and UM-UC-3, which were derived from high-grade urothelial carcinoma and have acquired mutations in *TP53* (40–42). As a control, we used the RT4 cell line, which originated from a benign urothelial papilloma and expresses wild-type *TP53* (43). Baseline evaluation showed detectable levels of phospho-Aurora A in all cell lines by both immunofluorescent localization and Western blot analysis (Fig. 2A and B). Application of 10 nmol/L to 1 μmol/L MLN8237 resulted in a loss of phospho-Aurora A at the mitotic spindle (Fig. 2A) and a dose-dependent reduction in phosphorylation of Aurora A (Fig. 2B). Application of MLN8237 did not affect total Aurora A levels and did not seem to alter Aurora B status within the cells as measured by phospho-histone-H3 expression as an indicator of Aurora B function (Fig. 2B).

Next, we used flow cytometry to assess the effect of MLN8237 on cell-cycle dynamics. Treatment of T24, UM-UC-3, and RT4 cells with 10 nmol/L to 1 μmol/L MLN8237 for 48 hours induced significant cell-cycle arrest in a dose-dependent manner (Fig. 2C). Considering only nonpolyploid cells (DNA content $\leq$ 4N), the proportion of cells with 4N DNA content increased from 9% with no treatment to 72% with 1 μmol/L MLN8237 in T24 cells, from 10% to 84% in UM-UC-3 cells, and from 22% to 92% in RT4 cells. This is consistent with a G_2–M arrest or a G_1 tetraploid cell population. Moreover, MLN8237 induced a significant increase in aneuploidy in the malignant T24 and UM-UC-3 cell lines but no increase in aneuploidy in the benign RT4 cell line. The proportion of all cells that were aneuploid (DNA content > 4N) increased from 17% with no treatment to 54% with 1 μmol/L MLN8237 in T24 cells and from 10% to 89% in UM-UC-3 cells but remained stable in RT4 cells.

MLN8237 induces distinct cellular phenotypes in benign and malignant bladder cells

To further characterize the phenotype of Aurora A inhibition, we used microscopy to visualize the cellular phenotype and mitotic spindle during cell-cycle arrest induced by MLN8237. Treatment of malignant T24 cells with 100 nmol/L MLN8237 for 24 hours resulted in a significant increase in cell size, whereas treatment of RT4 cells had no apparent effect on cell size (Fig. 3A). In addition, a minority of T24 cells appeared morphologically to be in mitotic arrest, with rounded cell morphology, condensed DNA, and multipolar spindles (Fig. 3B). Both cell lines showed disruption of the mitotic spindle and formation of aberrant multipolar spindle apparatuses following MLN8237 treatment (Fig. 3B).

T24 and RT4 cells were also triple-stained with tubulin, CENP-A, and DAPI and imaged with immunofluorescence microscopy. CENP-A staining was used to estimate relative centromere number and thus compare ploidy between treated and untreated cells. MLN8237-treated T24 cells showed markedly increased DNA content and CENP-A staining per cell, whereas RT4 cells did not (Fig. 3C). These results are consistent with the flow cytometry analysis that showed increases in aneuploidy with MLN8237 treatment in the malignant T24 cell line.

Immunofluorescent staining for total Aurora A showed expected localization of the protein to mitotic spindles under baseline conditions in both RT4 and T24 cells (Fig. 3D). However, inhibition of Aurora A activity with 100 nmol/L MLN8237 resulted in enhanced expression of Aurora A in the malignant T24 cells only, with augmentation of Aurora A expression both at the mitotic spindle and within the cytoplasm, although the mechanism behind this finding is unclear.

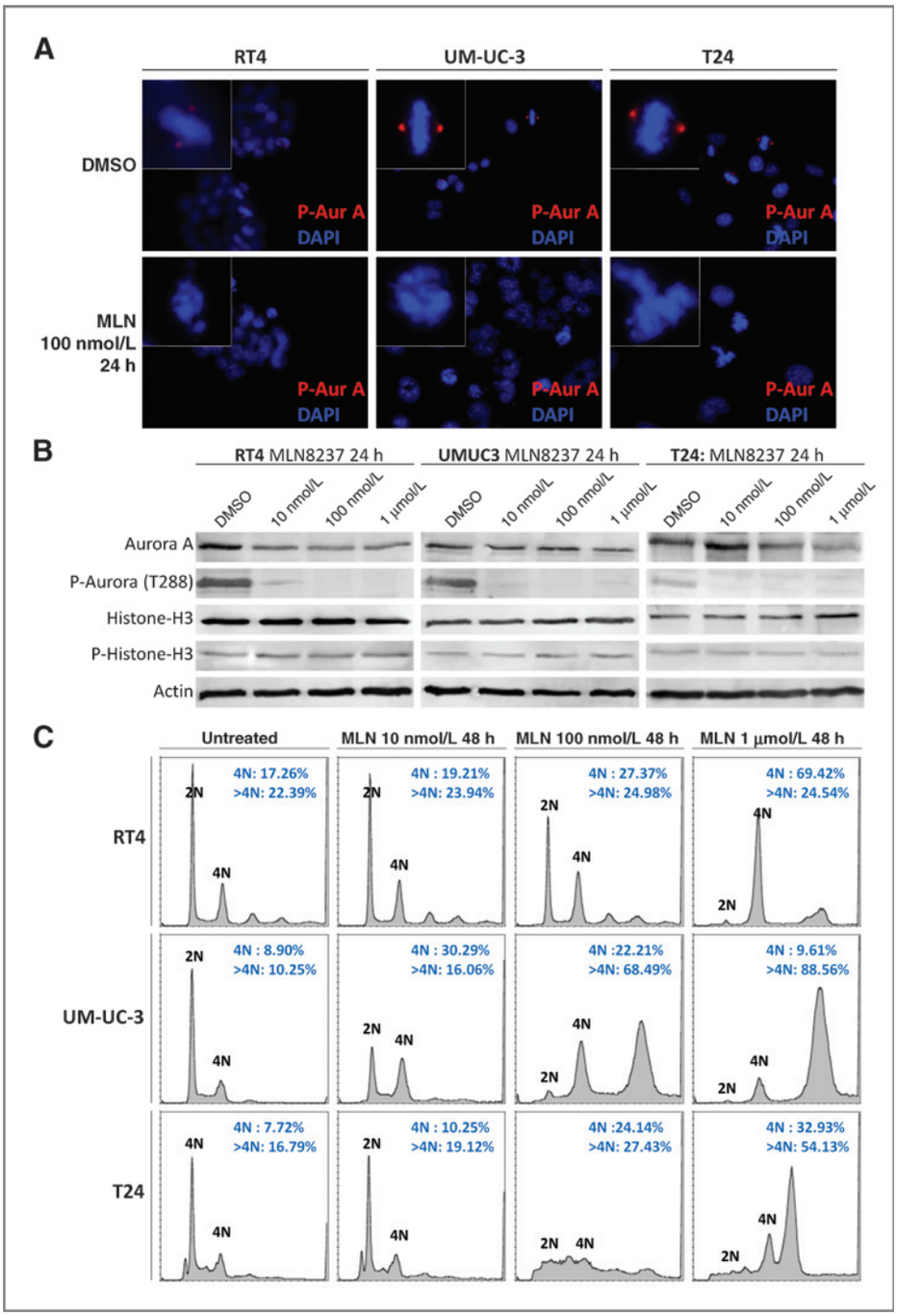

Figure 2. MLN8237 (MLN) induces cell-cycle arrest and aneuploidy of bladder cancer cell lines. A, MLN8237 inhibited expression of phospho-Aurora A-T288 at mitotic spindles. B, MLN8237 showed specificity for inhibiting Aurora A, as expression of histone-H3 and phospho-histone-H3, markers of Aurora B function, was maintained. C, PI staining with flow cytometry analysis was conducted to assess cell-cycle changes. T24, UM-UC-3, and RT4 cells were treated with 10 nmol/L to 1 μmol/L MLN8237 for 48 hours. All 3 cell lines showed dramatic cell-cycle arrest and increase in the 4N cell population in a dose-dependent manner. T24 and UM-UC-3 cells also showed a considerable increase in aneuploidy, whereas RT4 cells did not.

Finally, time-lapse microscopy was conducted to further visualize cell division dynamics following MLN8237 treatment. T24 cells treated with 100 nmol/L MLN8237 exhibited repeated attempts at mitosis within a 24-hour period with no increase in cell number over time (i.e., unsuccessful cytokinesis), resulting in a dramatic increase in cell size (Fig. 3E). Treated RT4 cells, in contrast, seemed to arrest shortly after the first attempt at mitosis, with no subsequent increase in cell size. Taken together, these results show that repeated cell-cycle progressions despite failure in separation of daughter cells in malignant T24 cells, but not benign RT4 cells, account for the development of aneuploidy in the former cell line following MLN8237 treatment.

Cytotoxicity and differential apoptotic processes mediate MLN8237's effects

Given the dramatic cell-cycle arrest caused by MLN8237, we sought to quantify growth inhibition induced by this compound in our cell lines. MLN8237 was administered at concentrations ranging from 0.316 nmol/L to 3.16 μmol/L to

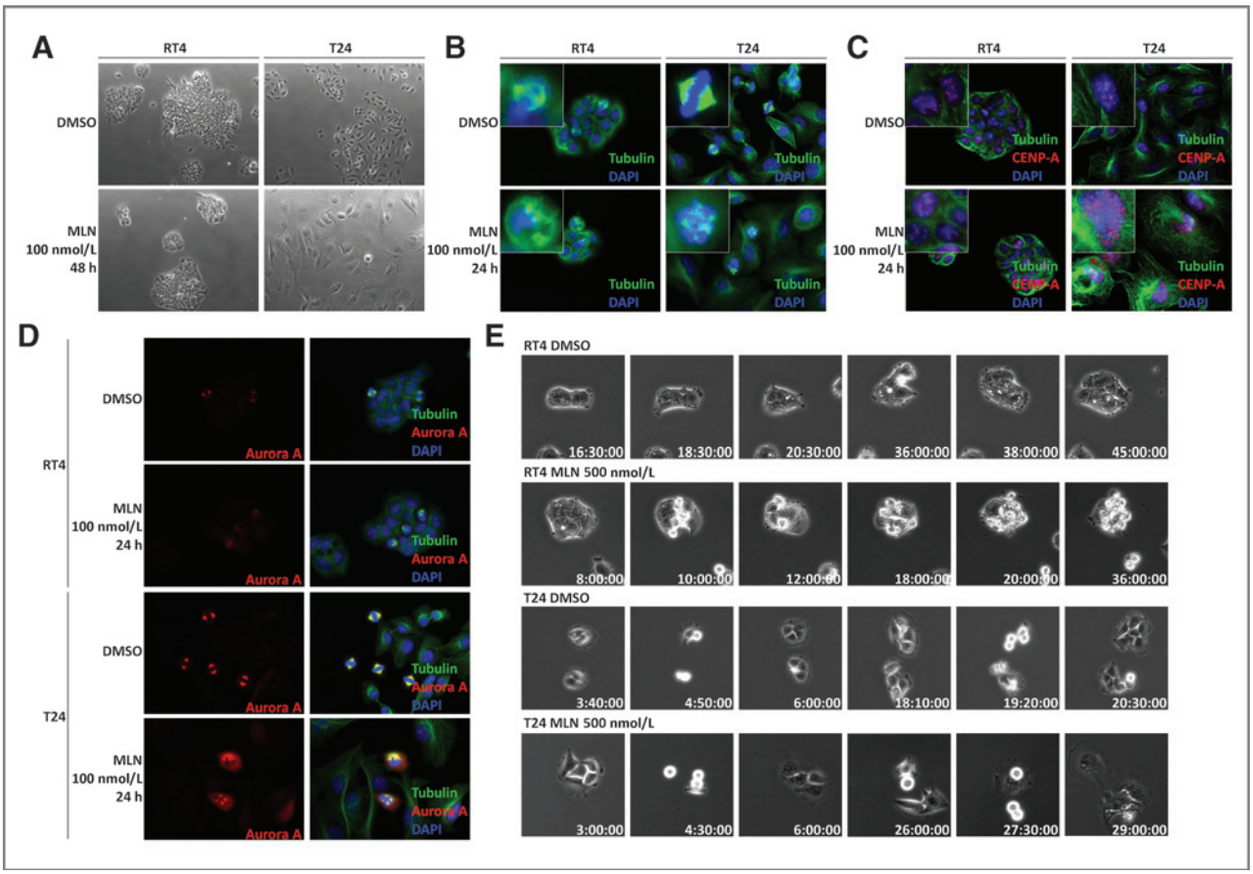

Figure 3. Cellular phenotypes of T24 and RT4 cells differ after MLN8237 (MLN) treatment. A, MLN8237 induces a dramatic increase in cell size in T24 cells but not RT4 cells. B, immunocytochemistry and fluorescence microscopy of T24 and RT4 cells revealed the formation of aberrant spindle figures upon MLN8237 treatment, with multipolar spindle apparatuses and failure of localization of chromatids to a single metaphase plate. C, T24 cells show a phenotype of increased cell size and ploidy, whereas RT4 cells do not. D, T24 cells also exhibit a subpopulation of cells exhibiting marked cytoplasmic Aurora A expression, whereas RT4 cells lacked cytoplasmic Aurora A expression. E, real-time imaging of T24 and RT4 cells treated with MLN8237 was conducted over 48 hours. T24 cells exhibited dramatic increases in cell size as a result of repeated cell-cycle progressions without separation of daughter cells. RT4 cells seemed to become arrested after one failed mitotic attempt, preventing repeated cell-cycle progressions that could otherwise result in increased ploidy.

T24, UM-UC-3, and RT4 cells for 96 hours (Fig. 4A). MTS assay was used to quantify cell viability, with individual data points expressed as relative standardized absorbance compared with untreated controls. MLN8237 was most potent in T24 and UM-UC-3 cells (IC_{50} of 31 and 45 nmol/L, respectively) and least potent in RT4 cells (IC_{50} of 120 nmol/L).

To assess apoptosis, we evaluated protein expression of cleaved PARP, p53, p21, and p73 in RT4 and T24 cells. Application of 100 nmol/L MLN8237 resulted in an increase in PARP cleavage expression in RT4 and T24 cells by 24 hours. RT4 cell lines, which contain wild-type p53, showed a peak in p53 expression at 24 hours after initiation of MLN8237 treatment, with a subsequent increase in the expression of p21, a downstream mediator of p53, through 72 hours (Fig. 4B). In contrast, T24 cells contain mutated p53; in this cell line an increase in p73 expression was apparent at 24 hours, whereas p53 and p21 expression remained unaltered.

To quantify apoptosis, annexin V staining and flow cytometry were conducted on T24 and RT4 cells. Both cell lines showed an increase in the apoptotic cell population starting at 24 hours after initiation of MLN8237 treatment, although this population was greater in the T24 cells (Fig. 4C). Thus, T24 cells seem to be more sensitive to MLN8237 as shown by the combination of a lower IC_{50} and a more sizeable apoptotic response as measured by annexin V staining (Fig. 4A and C).

Finally, to assess long-term viability posttreatment, clonogenic assays were conducted on RT4 and T24 cells. Treatment of both T24 and RT4 cells with 100 nmol/L MLN8237 for 48 hours resulted in less than 10% of cells maintaining capability to form clones in either cell line, and less than 1% clonogenic capability was detected in T24 or RT4 cells treated with 1 μmol/L MLN8237 (Fig. 4D).

MLN8237 inhibits tumor growth in mouse xenograft models

To assess the capacity of MLN8237 to reduce tumor growth *in vivo*, nude mice were inoculated with T24 cells in the subcutaneous flank tissue to induce growth of tumors

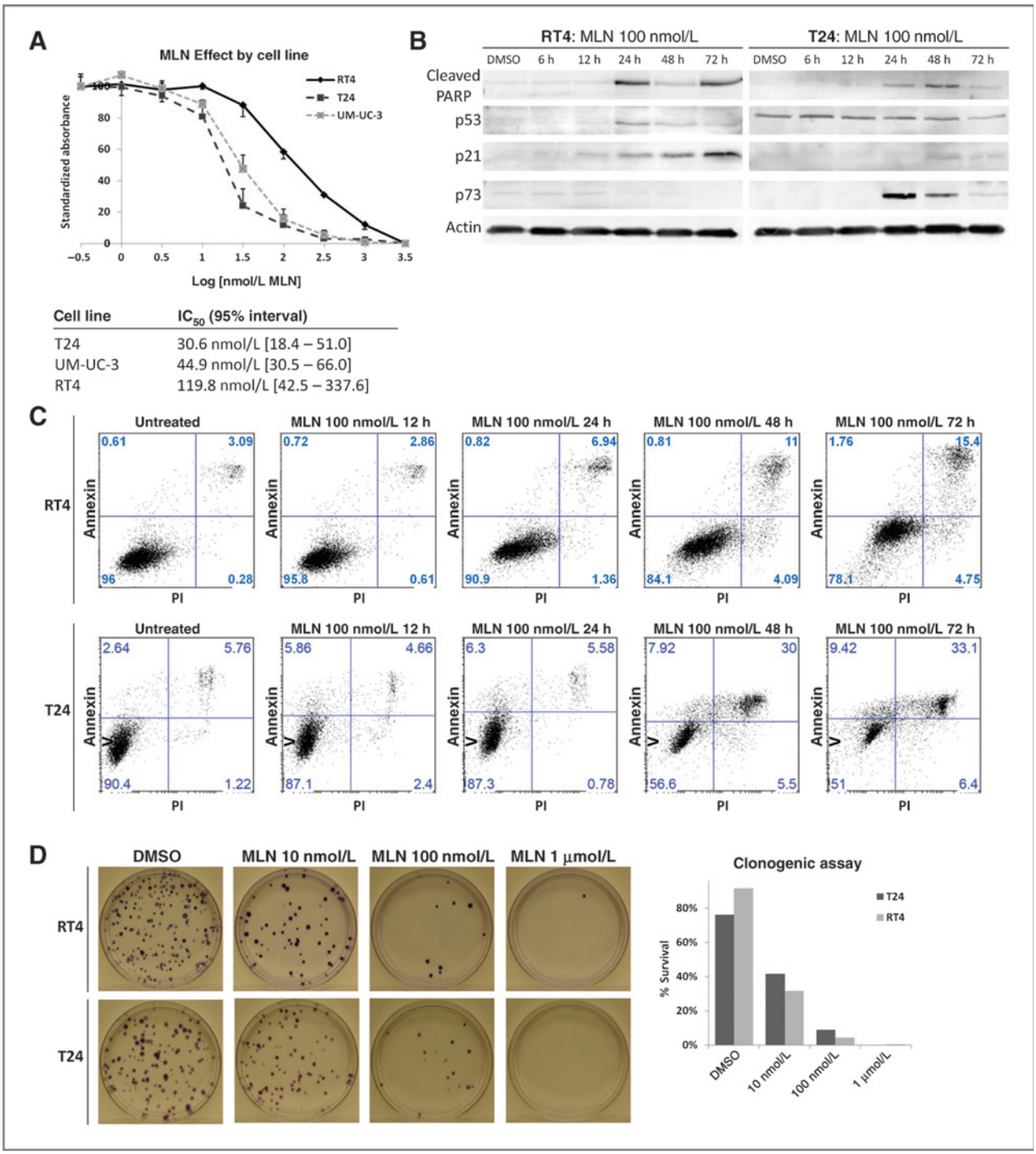

Figure 4. MLN8237 (MLN) induces cytotoxicity and differential apoptotic processes. A, MTS assay was used to calculate IC_{50} values for each cell line following treatment over a range of MLN8237 concentrations for 48 hours. MLN8237 exhibited highest potency in T24 and UM-UC-3 cells (IC_{50} of 31 and 45 nmol/L, respectively) and lowest potency in RT4 cells (IC_{50} of 120 nmol/L). B, Western blot analysis of T24 and RT4 cells for apoptotic markers revealed induction of p53 expression in RT4 cells, and induction of p73, but not p53, expression in T24 cells. Both cell lines showed increased expression of the apoptotic marker cleaved PARP starting 24 hours after initiation of treatment. C, annexin V staining with flow cytometry analysis of T24 and RT4 cells revealed an increased apoptotic cell fraction at 48 and 72 hours after initiation of MLN8237 treatment. D, clonogenic assays of T24 and RT4 cells showed 90% inhibition of long-term clone forming capability at 100 nmol/L MLN8237.

($N = 8$ for treatment group, $N = 8$ for control group). When tumor sizes reached 250 mm^3, a 4-week regimen of MLN8237 30 mg/kg orally 5 times weekly was initiated. No statistically significant difference in tumor size between the control and treatment groups was noted at initiation of treatment (t test; $P > 0.05$). Mice treated with MLN8237

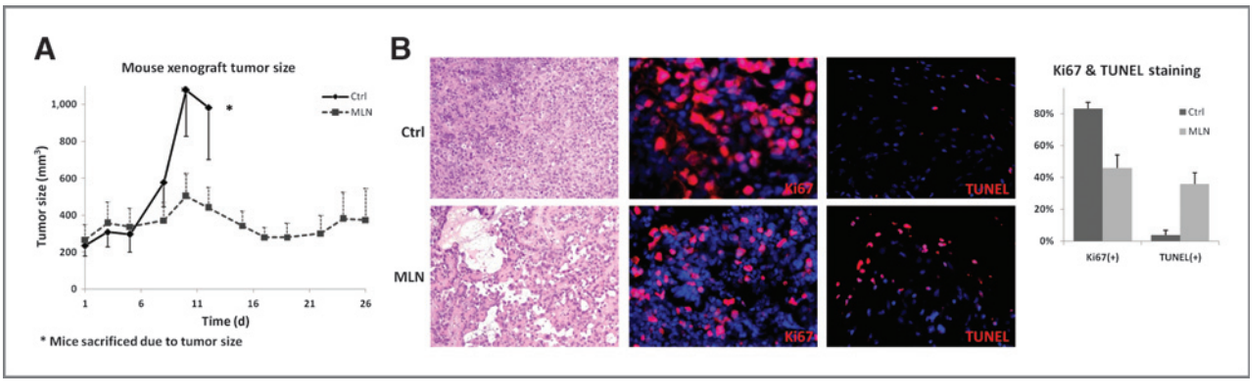

Figure 5. MLN8237 (MLN) arrests tumor growth *in vivo* in a mouse xenograft model. A, mice were treated with the drug at 30 mg/kg doses orally once daily for 4 weeks, and tumor volumes over time were charted. Mice in the treatment group showed arrest of tumor growth throughout the 4-week treatment regimen. Vehicle-treated control mice, on the other hand, showed a dramatic increase in tumor size, and all but 1 control mice were sacrificed by day 15 due to tumor size. B, tumors were harvested and stained for hematoxylin and eosin, Ki67 for proliferation, and TUNEL for apoptosis. Tumors treated with MLN8237 showed decreased cellularity and regions of cell death and fibrosis, as well as decreased Ki67 staining and increased TUNEL staining, compared with tumors from control mice. Percentage of cells staining positive for Ki67 and TUNEL were counted in 5 visual fields per group and depicted in the bar graph.

exhibited arrest of tumor growth compared with the control group (Wilcoxon rank-sum; $P < 0.05$) and showed no statistically significant difference in tumor size between initiation of treatment and completion of the 4-week regimen (t test; $P > 0.05$; Fig. 5A). In contrast, untreated control mice exhibited dramatic increases in tumor growth, with tumor sizes quadrupling within 2 weeks of initial treatment. Because of the rapid rate of tumor growth in the control population, this experimental group was terminated by day 15 of treatment.

To further illustrate the antitumor activity of MLN8237 *in vivo*, tumors were harvested and stained with hematoxylin and eosin, Ki67, and terminal deoxynucleotidyl transferase–mediated dUTP nick end labeling (TUNEL). Tumors treated with MLN8237 showed decreased cellularity compared with tumors from control mice, as well as regions of cell death and fibrosis (Fig. 5B). The MLN8237-treated group also exhibited a 50% decrease in percentage of cells staining positive for Ki67 and a 10-fold increase in percentage of cells staining positive for TUNEL (t test; $P < 0.05$; Fig. 5B).

MLN8237 exhibits schedule-dependent synergism with paclitaxel and gemcitabine *in vitro*

Finally, we evaluated the response of the T24 bladder cancer cell line to MLN8237 in combination with either paclitaxel or gemcitabine—2 agents currently used for the treatment of advanced bladder cancer. Drugs were administered either simultaneously for 48 hours, or sequentially, with one drug for 48 hours, followed by washout and immediate addition of the other drug for 48 hours. MTS assay was used to quantify cell viability and combination indices were calculated to determine synergism or antagonism. Effects of combination treatments were compared with control treatments with a single drug.

Combination treatments showed the greatest reduction in cell viability when drugs were dosed sequentially. Sequential administration of MLN8237 followed by either paclitaxel or gemcitabine resulted in synergistic interactions, most prominently at lower concentrations of the second drug (Fig. 6). For example, when paclitaxel was administered alone, 1.6 nmol/L paclitaxel produced 30% of maximal reduction in cell viability, but when paclitaxel was administered after 100 nmol/L MLN8237, 1.6 nmol/L paclitaxel achieved 70% of maximal reduction in cell viability. Likewise, 4 nmol/L gemcitabine alone produced 48% of maximal reduction in cell viability, whereas 4 nmol/L gemcitabine administered sequentially following 100 nmol/L MLN8237 was able to achieve 87% of maximal reduction in cell viability. Sequential administration of either paclitaxel or gemcitabine followed by MLN8237 resulted in largely additive effects. Notably, MLN8237 was much less effective when concurrently administered with either paclitaxel or gemcitabine, as simultaneous administration of MLN8237 with either paclitaxel or gemcitabine produced largely antagonistic effects.

To further show that combination treatments are cytotoxic and inhibit cell viability, the percentage of cells staining positive for Trypan blue was computed. Combination treatments resulted in increased percentage of cells staining positive for Trypan blue, with sequential dosing regimens having the greatest effect (Supplementary Fig. S1). Finally, we used flow cytometry to evaluate the effects of combination regimens on the cell cycle. For both MLN8237/paclitaxel and MLN8237/gemcitabine combinations, sequential dosing regimens produced the most significant extent of cell-cycle arrest, whereas simultaneous dosing regimens were the least effective in causing additional cell-cycle arrest (Supplementary Fig. S2). For example, sequential administrations of MLN8237 and paclitaxel produced a broad aneuploid cell population with no predominance of a single ploidy, whereas simultaneous MLN8237 and paclitaxel administration resulted in a cell-cycle profile indistinguishable from that of MLN8237 treatment alone.

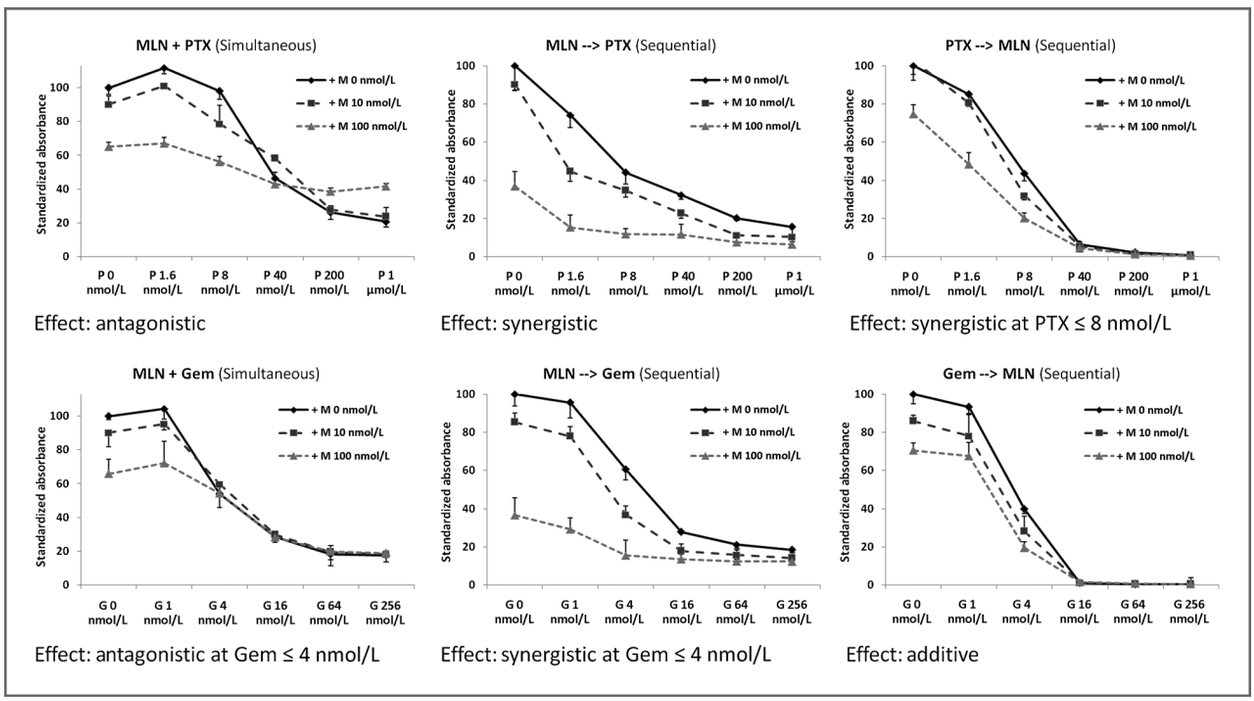

Figure 6. Interactions of MLN8237 with paclitaxel and gemcitabine *in vitro* are schedule-dependent. MLN8237 (MLN) was combined with either paclitaxel (PTX) or gemcitabine (Gem) in T24 cells. Drugs were administered either simultaneously for 48 hours (left), or sequentially, with one drug for 48 hours, followed by washout and the other drug for 48 hours (middle and right). MTS assay was used to quantify the effect on cell viability of these combination treatments. MLN8237 showed synergistic effects with paclitaxel and gemcitabine when dosed sequentially (middle and right), and antagonistic effects when dosed simultaneously (left).

Discussion

Despite bladder cancer being the fourth most common cancer in men in the United States, the molecular processes that underlie its development are relatively understudied. To identify new putative drug targets, we compared gene expression profiles between normal urothelium and patients with muscle-invasive urothelial carcinoma and identified global upregulation of mitotic spindle-associated genes. While overexpression of the Aurora kinases in bladder cancer has been previously described, to our knowledge, this is the first report of a broad overexpression of mitotic spindle checkpoint components as a common characteristic of human bladder cancer. Although the Aurora kinases currently represent the most accessible therapeutic target among the genes we identified, other members of the mitotic spindle checkpoint may warrant further study as potential clinical biomarkers of disease or alternate drug targets.

With the goal of exploiting this pathway as anticancer therapy, we evaluated the impact of the Aurora kinase A inhibitor MLN8237 on bladder cancer cells *in vitro*. Application of MLN8237 to papilloma-derived RT4 cells and malignant T24 and UM-UC-3 urothelial carcinoma cells resulted in cell-cycle arrest, mitotic spindle failure, and eventual apoptotic cell death. Interestingly, Aurora A inhibition induced aneuploidy in malignant bladder cells but not in the RT4 cell line, we suspect due to intact p53 function in RT4 cells that allows for cell-cycle arrest following mitotic failure. This is in agreement with previous reports of activation of a p53-dependent postmitotic checkpoint as a mechanism of preventing aneuploidy if the spindle checkpoint fails (44–46). In contrast, increased p73 expression seems to drive apoptosis in the p53-deficient T24 cell line. Our results are consistent with a previous report of p73-dependent apoptosis following Aurora A inhibition in p53 mutant cells (47). Given the high incidence of p53 mutations in human bladder cancer, activation of an alternate apoptotic pathway following Aurora A inhibition constitutes an important mechanism for achieving cell death. In addition, the differential IC_{50} values suggest increased potency of Aurora kinase A inhibition in malignant cells, supporting the conclusion of higher sensitivity in these cells.

We also examined the ability of MLN8237 to provide efficacy as a component of a multidrug regimen. Simultaneous administration of MLN8237 and either paclitaxel or gemcitabine *in vitro* revealed an antagonistic relationship, whereas sequential administration resulted in a synergistic interaction. This is in agreement with previous reports of additive and synergistic effects when Aurora kinase inhibitors are sequentially dosed in combination with other agents, including nucleoside analogs and taxols (48–50). These results suggest that the induction of spindle checkpoint dysfunction by MLN8237 can potentiate the ability of paclitaxel and gemcitabine to induce cell-cycle arrest and underscore the potential of

MLN8237 as either an independent or concurrent agent in bladder cancer.

Finally, we showed the *in vivo* capacity of MLN8237 to arrest tumor growth in a mouse xenograft model of bladder cancer. In other studies, MLN8237 has been shown to have similar antitumor activity in animal models and in early clinical testing but has not been evaluated specifically in bladder cancer. Our demonstration of decreased tumor size, associated with cell drop-out and reduced proliferation index, following MLN8237 administration in a mouse xenograft model of bladder cancer is consistent with current published findings of tumor response to this drug. Nevertheless, we recognize that our *in vivo* model was limited to an evaluation of 8 tumors in a lone treatment group. We anticipate that a more expansive study in the future could delineate the varying antitumor effects of different dosages and of combination regimens.

The demand for improved pharmacologic options for bladder cancer represents a timely opportunity for testing Aurora kinase inhibitors in bladder cancer, either alone or in conjunction with currently established therapies. In this study, we identify spindle checkpoint dysregulation as a common feature of human urothelial carcinoma of the bladder. Targeting this pathway with the Aurora A inhibitor MLN8237 induced cell-cycle arrest, aneuploidy, spindle abnormalities, and apoptosis in bladder cancer cell lines, and arrested tumor growth in a mouse xenograft model. On the basis of these findings, we believe that the mitotic spindle checkpoint in human bladder cancer warrants further investigation to identify and characterize the mechanisms of spindle checkpoint failures that lead to tumorigenesis, and to explore the anticancer potential of drugs that target this pathway, including Aurora kinase inhibitors.

Disclosure of Potential Conflicts of Interest

No potential conflicts of interest were disclosed.

Authors' Contributions

Conception and design: N. Zhou, A. Almasan, D.E. Hansel
Development of methodology: N. Zhou, K. Singh, M.C. Mir, B.T. Teh, D.E. Hansel
Acquisition of data (provided animals, acquired and managed patients, provided facilities, etc.): N. Zhou, K. Singh, M.C. Mir, Y. Parker, D. Lindner, B.T. Teh, D.E. Hansel
Analysis and interpretation of data (e.g., statistical analysis, biostatistics, computational analysis): N. Zhou, K. Singh, D. Lindner, J.A. Ecsedy, Z. Zhang, B.T. Teh, A. Almasan, D.E. Hansel
Writing, review, and/or revision of the manuscript: N. Zhou, K. Singh, M. C. Mir, D. Lindner, R. Dreicer, J.A. Ecsedy, Z. Zhang, B.T. Teh, A. Almasan, D.E. Hansel
Administrative, technical, or material support (i.e., reporting or organizing data, constructing databases): N. Zhou, M.C. Mir, B.T. Teh, D.E. Hansel
Study supervision: R. Dreicer, B.T. Teh, D.E. Hansel

Grant Support

This work was supported by the Case Western Reserve University/Cleveland Clinic CTSA Grant Number UL1 RR024989 from the National Center for Research Resources (NCRR) and a KL2 career development award (RR024990) to D.E. Hansel.

The costs of publication of this article were defrayed in part by the payment of page charges. This article must therefore be hereby marked *advertisement* in accordance with 18 U.S.C. Section 1734 solely to indicate this fact.

Received August 1, 2012; revised December 17, 2012; accepted January 21, 2013; published OnlineFirst February 12, 2013.

References

1. Dar AA, Goff LW, Majid S, Berlin J, El-Rifai W. Aurora kinase inhibitors—rising stars in cancer therapeutics? Mol Cancer Ther 2010; 9:268–78.
2. Karthigeyan D, Prasad SB, Shandilya J, Agrawal S, Kundu TK. Biology of Aurora A kinase: implications in cancer manifestation and therapy. Med Res Rev. 2010 Mar 1. [Epub ahead of print].
3. Marumoto T, Zhang D, Saya H. Aurora-A—a guardian of poles. Nat Rev Cancer 2005;5:42–50.
4. Carmena M, Earnshaw WC. The cellular geography of Aurora kinases. Nat Rev Mol Cell Biol 2003;4:842–54.
5. Slattery SD, Mancini MA, Brinkley BR, Hall RM. Aurora-C kinase supports mitotic progression in the absence of Aurora-B. Cell Cycle 2009;8:2984–94.
6. Sesai K, Katayama H, Stenoien DL, Fujii S, Honda R, Kimura M, et al. Aurora-C kinase is a novel chromosomal passenger protein that can complement Aurora-B kinase function in mitotic cells. Cell Motil Cytoskeleton 2004;59:249–63.
7. Bufo P, Sanguedolce F, Tortorella S, Cormio L, Carrieri G, Pannone G. Expression of mitotic kinases phospho-Aurora A and Aurora B correlates with clinical and pathological parameters in bladder neoplasms. Histol Histopathol 2010;25:1371–7.
8. Comperat E, Bieche I, Dargere D, Laurendeau I, Vieillefond A, Benoit G, et al. Gene expression study of Aurora A reveals implication during bladder carcinogenesis and increasing values in invasive urothelial cancer. Urology 2008;72:873–7.
9. Comperat E, Camparo P, Haus R, Chartier-Kastler E, Radenen B, Richard F, et al. Aurora-A/STK15 is a predictive factor for recurrent behaviour in non-invasive bladder carcinoma: a study of 128 cases of non-invasive neoplasms. Virchows Arch 2007;450:419–24.
10. Baba Y, Nosho K, Shima K, Irahara N, Kure S, Toyoda S, et al. Aurora-A expression is independently associated with chromosomal instability in colorectal cancer. Neoplasia 2009;11:418–25.
11. Mhawech-Fauceglia P, Fischer G, Beck A, Cheney RT, Hermann FR. Raf1, Aurora-A/STK15 and E-cadherin biomarkers expression in patients with pTa/pT1 urothelial bladder carcinoma; a retrospective TMA study of 246 patients with long-term follow-up. Euro J Surg Oncol 2006;32:439–44.
12. Kops GJ, Weaver BA, Cleveland DW. On the road to cancer: aneuploidy and the mitotic checkpoint. Nat Rev Cancer 2005;5:773–85.
13. Anand S, Penrhyn-Lowe S, Venkitaraman AR. Aurora-A amplification overrides the mitotic spindle assembly checkpoint, including resistance to taxol. Cancer Cell 2003;3:51–62.
14. Wang X, Zhou YX, Qiao W, Tominaga Y, Ouchi M, Ouchi T, et al. Overexpression of Aurora kinase A in mouse mammary epithelium induces genetic instability preceding mammary tumor formation. Oncogene 2006;25:7148–58.
15. Zhou H, Kuang J, Zhong L, Kuo WL, Gray JW, Sahin A, et al. Tumor amplified kinase STK15/BTAK induces centrosome amplification, aneuploidy, and transformation. Nat Genet 1998;20:189–93.
16. Goepfert TM, Adigun YE, Zhong L, Gay J, Medina D, Brinkley WR. Centrosome amplification and overexpression of Aurora A are early events in rat mammary carcinogenesis. Cancer Res 2002;62:4115–22.
17. Ota T, Suto S, Katayama H, Han ZB, Suzuki F, Maeda M, et al. Increased mitotic phosphorylation of histone H3 attributable to AIM-

1/Aurora-B overexpression contributes to chromosome number instability. Cancer Res 2002;62:5168–77.
18. Tatsuka M, Katayama H, Ota T, Tanaka T, Odashima S, Suzuki F, et al. Multinuclearity and increased ploidy caused by overexpression of the Aurora- and Ip1-like midbody-associated protein mitotic kinase in human cancer cells. Cancer Res 1998;58:4811–6.
19. Katayama H, Ota T, Jisaki F, Ueda Y, Tanaka T, Odashima S, et al. Mitotic kinase expression and colorectal cancer progression. J Natl Cancer Inst 1999;91:1160–2.
20. Lei Y, Yan S, Ming-De L, Na L, Rui-Fa H. Prognostic significance of Aurora-A expression in human bladder cancer. Acta Histochem 2011;113:514–8.
21. Tomita M, Mori N. Aurora A selective inhibitor MLN8237 suppresses the growth and survival of HLTV-1-infected T cells *in vitro*. Cancer Sci 2010;101:1204–11.
22. Kelly KR, Ecsedy J, Medina E, Mahalingam D, Padmanahan S, Nawrocki ST, et al. The novel Aurora A kinase inhibitor MLN8237 is active in resistant chronic myeloid leukemia and significantly increases the efficacy of nilotinib. J Cell Mol Med 2011;15:2057–70.
23. Gorgun G, Calabrese E, Hideshima T, Ecsedy J, Perrone G, Mani M, et al. A novel Aurora-A kinase inhibitor MLN8237 induces cytotoxicity and cell-cycle arrest in multiple myeloma. Blood 2010;115:5202–13.
24. Mahadeven D, Stejskal A, Cooke LS, Manziello A, Morales C, Persky DO, et al. Aurora A inhibitor (MLN8237) plus vincristine plus rituximab is synthetic lethal and a potential curative therapy in aggressive B-cell non-Hodgkin lymphoma. Clin Cancer Res 2012;18:2210–9.
25. Sehdev V, Peng D, Soutto M, Washington MK, Revetta F, Ecsedy J, et al. The aurora kinase inhibitor MLN8237 enhances cisplatin-induced cell death in esophageal adenocarcinoma cells. Mol Cancer Ther 2012;11:763–74.
26. Venkataraman S, Alimova I, Tello T, Harris PS, Knipstein JA, Donson AM, et al. Targeting Aurora kinase A enhances radiation sensitivity of atypical rhabdoid tumor cells. J Neurooncol 2012;107:517–26.
27. Siegel R, Naishadham D, Jemal A. Cancer statistics, 2012. CA Cancer J Clin 2012;62:10–29.
28. Pliarchopoulou K, Laschos K, Pectasides D. Current chemotherapeutic options for the treatment of advanced bladder cancer: a review. Urol Oncol. 2010 Sep 13. [Epub ahead of print].
29. Sternberg CN, de Mulder P, Schornagel JH, Theodore C, Fossa SD, van Oosterom AT, et al. Seven year update of an EORTC phase III trial of high-dose intensity M-VAC chemotherapy and G-CSF versus classic M-VAC in advanced urothelial tract tumours. Eur J Cancer 2006;42:50–4.
30. von der Masse H, Hansen SW, Roberts JT, Dogliotti L, Oliver T, Moore MJ, et al. Gemcitabine and cisplatin versus methotrexate, vinblastine, doxorubicin, and cisplatin in advanced or metastatic bladder cancer: results of a large, randomized, multinational, multicenter, phase III study. J Clin Oncol 2000;18:3068–77.
31. Garcia JA, Dreicer R. Systemic chemotherapy for advanced bladder cancer: update and controversies. J Clin Oncol 2006;24:5545–51.
32. Dai M, Wang P, Boyd AD, Kostov G, Athey B, Jones EG, et al. Evolving gene/transcript definitions significantly alter the interpretation of GeneChip data. Nucleic Acids Res 2005;33:e175.
33. Gautier L, Cope L, Bolstad BM, Irizarry RA. Affy—analysis of Affymetrix GeneChip data at the probe level. Bioinformatics 2004;20:307–15.
34. Irizarry RA, Bolstad BM, Collin F, Cope LM, Hobbs B, Speed TP. Summaries of Affymetrix GeneChip probe level data. Nucleic Acids Res 2003;31:e15.
35. Irizarry RA, Hobbs B, Collin F, Beazer-Barclay YD, Antonellis KJ, Scherf U, et al. Exploration, normalization, and summaries of high density oligonucleotide array probe level data. Biostatistics 2003;4:249–64.
36. Bolstad BM, Irizarry RA, Astrand M, Speed TP. A comparison of normalization methods for high density oligonucleotide array data based on variance and bias. Bioinformatics 2003;19:185–93.
37. Hansel DE, Platt E, Orloff M, Harwalker J, Sethu S, Hicks JL, et al. Mammalian target of rapamycin (mTOR) regulates cellular proliferation and tumor growth in urothelial carcinoma. Am J Pathol 2010;176:3062–72.
38. Chou TC. Drug combination studies and their synergy quantification using the Chou-Talalay method. Cancer Res 2010;70:440–6.
39. Edgar R, Domrachev M, Lash AE. Gene Expression Omnibus: NCBI gene expression and hybridization array data repository. Nucleic Acid Res 2002;30:207–10.
40. da Silva GN, de Castro Marcondes JP, de Camargo EA, da Silva Passos Junior GA, Sakamoto-Hojo ET, Salvadori DM. Cell cycle arrest and apoptosis in TP53 subtypes of bladder carcinoma cell lines treated with cisplatin and gemcitabine. Exp Biol Med (Maywood) 2010;235:814–24.
41. Stravopodis DJ, Karkoulis PK, Konstantakou EG, Melachroinou S, Thanasopoulou A, Aravantinos G, et al. Thymidylate synthase inhibition induces p53-dependent and p53-independent apoptotic responses in human urinary bladder cancer cells. J Cancer Res Clin Oncol 2011;137:359–74.
42. Cooper MJ, Haluschak JJ, Johnson D, Schwartz S, Morrison LJ, Lippa M, et al. p53 mutations in bladder carcinoma cell lines. Oncol Res 1994;6:569–79.
43. Puzio-Kuter AM, Castillo-Martin M, Kinkade CW, Wang X, Shen TH, Matos T, et al. Inactivation of p53 and Pten promotes invasive bladder cancer. Genes Dev 2009;23:675–80.
44. Tsuchiya M, Katagiri N, Kuroda T, Kishimoto H, Nishimura K, Kumazawa T, et al. Critical role of the nucleolus in activation of the p53-dependent postmitotic checkpoint. Biochem Biophys Res Commun 2011;407:378–82.
45. Li M, Fang X, Baker DJ, Guo L, Gao X, Wei Z, et al. The ATM-p53 pathway suppresses aneuploidy-induced tumorigenesis. Proc Natl Acad Sci U S A 2010;107:14188–93.
46. Huang YF, Chang MD, Shieh SY. TTK/hMps1 mediates the p53-dependent postmitotic checkpoint by phosphorylating p53 at Thr18. Mol Cell Biol 2009;29:2935–44.
47. Dar AA, Belkhiri A, Ecsedy J, Zaika A, El-Rifai W. Aurora kinase A inhibition leads to p73-dependent apoptosis in p53-deficient cancer cells. Cancer Res 2008;68:8998–9004.
48. Qi W, Cooke LS, Liu X, Rimsza L, Roe DJ, Manziolli A, et al. Aurora inhibitor MLN8237 in combination with docetaxel enhances apoptosis and anti-tumor activity in mantle cell lymphoma. Biochem Pharmacol 2011;87:881–90.
49. VanderPorten EC, Taverna P, Hogan JN, Ballinger MD, Flanagan WM, Fucini RV. The Aurora kinase inhibitor SNS-314 shows broad therapeutic potential with chemotherapeutics and synergy with microtubule-targeted agents in a colon carcinoma model. Mol Cancer Ther 2009;8:930–9.
50. Kelly KR, Nawrocki ST, Espitia CM, Zhang M, Yang JJ, Padmanabhan S, et al. Targeting Aurora A kinase activity with the investigational agent alisertib increases the efficacy of cytarabine through a FOXO-dependent mechanism. Int J Cancer 2012;131:2693–703.